Engineered Biosynthesis of Novel Polyketides: Stereochemical Course of Two Reactions Catalyzed by a Polyketide Synthase†

Hong Fu,‡ Robert McDaniel,‡ David A. Hopwood,§ and Chaitan Khosla*,‡

Department of Chemical Engineering, Stanford University, Stanford, California 94305-5025, and Department of Genetics, John Innes Centre, Norwich NR4 7UH, U.K.

Received February 21, 1994; Revised Manuscript Received May 9, 1994®

ABSTRACT: A genetically engineered strain expressing the essential components of the tetracenomycin polyketide synthase (*tcm* PKS) along with the actinorhodin ketoreductase (*act* KR) was found to produce two new (diastereomeric) aromatic polyketides, designated RM20b and RM20c, in addition to RM20, whose structure was reported earlier [McDaniel, R., Ebert-Khosla, S., Hopwood, D. A., & Khosla, C. (1993) *Science 262*, 1546–1550]. Spectroscopic and *in vivo* isotopic labeling analysis of RM20b and RM20c revealed that their polyketide backbones were identical to that of RM20 with respect to chain length, regiospecificity of ketoreduction, and regiospecificity of the first intramolecular aldol condensation. This is consistent with earlier predictions that the essential components of the PKS—a bifunctional ketosynthase/acyltransferase, a chain length determining factor, and an acyl carrier protein—are responsible for controlling each of these features of the polyketide backbone [McDaniel, R., Ebert-Khosla, S., Hopwood, D. A., & Khosla, C. (1993) *Science 262*, 1546–1550; McDaniel, R., Ebert-Khosla, S., Hopwood, D. A., & Khosla, C. (1993) *J. Am. Chem. Soc. 115*, 11671–11675; Fu, H., Ebert-Khosla, S., Hopwood, D. A., & Khosla, C. (1994) *J. Am. Chem. Soc. 116*, 4166–4170]. In addition, however, RM20b and RM20c possess two unusual features. In both molecules the hydroxyls on sp^3 C-9 and C-7 of the first six-membered ring, which arise as a result of ketoreduction and aldol condensation, respectively, are intact, rather than being lost via dehydration. Furthermore, the relative yield of RM20b (in which these hydroxyls are *syn*) is 7-fold greater than that of RM20c (in which they are *anti*). The novelty of RM20b and RM20c is indicative of the catalytic flexibility of recombinant PKSs and has encouraging implications for the generation of novel polyketides through the manipulation of gene structure and organization.

Polyketides are a large family of structurally diverse natural products possessing a broad range of biological activities, including antibiotic and pharmacological properties. Biosynthetic and molecular genetic studies have demonstrated that polyketide synthases (PKSs)[1] are structurally and mechanistically related to each other and to fatty acid synthases (FASs) (O'Hagan, 1991; Katz & Donadio, 1993). The PKSs are multifunctional enzymes that catalyze repeated (decarboxylative) Claisen condensations between acyl thioesters (usually acetyl, propionyl, malonyl, or methylmalonyl). After the carbon chain has grown to a length characteristic of each specific product, it is released from the synthase by thiolysis or acyl transfer. Unlike typical FASs, PKSs introduce structural variability into the product by varying the extent of the reductive cycle comprising a ketoreduction, dehydration, and enoyl reduction on each β-keto group of the polyketide chain.

An important scientific challenge is to understand the structural basis for the exquisite catalytic specificity of each multifunctional PKS. For example, both the PKSs involved in the biosynthesis of actinorhodin (**1**) and tetracenomycin (**2**) specifically utilize acetate primer units and malonate extender units. The actinorhodin (*act*) PKS catalyzes chain termination following seven condensation cycles, whereas the tetracenomycin (*tcm*) PKS catalyzes chain termination after nine condensation cycles. The degree of reduction and the regiochemistry of cyclization of the two polyketide backbones also reflect differences between the catalytic specificities of the two PKSs. While some of these differences can be rationalized based upon the presence or absence of specific genes within the PKS gene clusters—for example, the *tcm* PKS gene cluster, which produces an unreduced polyketide, lacks a ketoreductase gene (Figure 1)—most differences in specificities probably arise due to more subtle structural differences between the two PKSs.

As a first step toward understanding how PKSs achieve their high degree of specificity, we have developed a recombinant system for combinatorially expressing PKS subunits obtained from different gene clusters (such as the *act* and the *tcm* PKS gene clusters, shown in Figure 1) (McDaniel et al., 1993a). Structural analysis of novel molecules produced by these recombinant organisms enables one to identify the subunit(s) responsible for controlling the specificity of individual reactions within the overall catalytic cycle. It was already reported that (McDaniel et al., 1993a,b; Fu et al., 1994): (i) the chain length is, at least in part, dictated by a specific protein, which was therefore called the chain length determining factor (CLF; Figure 1); (ii) some heterologous ketosynthase/putative acyl transferase (KS/AT; Figure 1). CLF pairs gave rise to functional PKSs, but other pairs were nonfunctional; (iii) acyl carrier proteins (ACPs; Figure 1) could be interchanged among different synthases without affecting product structure; (iv) a specific ketoreductase (the

† This research was supported in part by grants from the National Science Foundation (BCS-9209901), the American Cancer Society (IRG-32-34), and the Camille and Henry Dreyfus Foundation to C.K. D.A.H. acknowledges financial support from the Agricultural and Food Research Council and the John Innes Foundation.

* Author to whom correspondence should be addressed.

‡ Stanford University.

§ John Innes Centre.

® Abstract published in *Advance ACS Abstracts*, July 1, 1994.

[1] Abbreviations: PKS, polyketide synthase; FAS, fatty acid synthase; KR, ketoreductase; KS, ketosynthase; AT, acyltransferase; CLF, chain length determining factor; ACP, acyl carrier protein; CYC, cyclase.

0006-2960/94/0433-9321$04.50/0

Table 1: ^1H and ^{13}C NMR Data for RM20b (**5**) and RM20c (**6**)[a]

	RM20b (**5**)			RM20c (**6**)		
carbon[b]	^{13}C δ (ppm)[c]	J_{cc}(Hz)[c]	^1H δ (ppm)	carbon	^{13}C δ (ppm)	^1H δ (ppm)
1	163.5 (164.5)	79.6 (80.0)	11.80 (s, 10H)	1	162.8	11.70 (s, 10H)
2	89.0 (89.8)	79.0 (79.0)	5.35 (s, 1H)	2	88.8	5.38 (s, 1H)
3	182.2 (183.5)	58.3 (59.8)		3	179.3	
4	102.9 (103.9)	58.0 (58.3)	5.96 (s, 1H)	4	102.6	6.00 (s, 1H)
5	161.4	50.8		5	161.1	
6	41.3 (41.9)	51.4 (51.2)	3.19 (d, J = 15.0 Hz, 1H); 2.80 (d, J = 14.9 Hz), 1H)	6	43.7	3.19 (d, J = 13.9 Hz, 1H); 2.96 (d, J = 13.9 Hz, 1H)
7	78.2 (79.2)	38.3 (38.7)	16.18 (s, 10H)	7	72.7	6.14 (s, 10H)
8	41.6 (42.5)	38.3 (38.5)	2.45 (dd, J = 11.9/2.5 Hz, 1H); 1.94 (dd, J = 12.1/12.1 Hz, 1H)	8	44.2	2.28 (dd, J = 11.6/2.2 Hz, 1H); 1.78 (dd, J = 12.2/12.2 Hz, 1H)
9	60.9 (62.2)	36.7 (36.7)	4.21 (m, 1H), 5.36 (s, 10H)	9	61.2	4.16 (m, 1H), 5.38 (s, 10H)
10	(40.8)	(37.7)	2.82 (dd, J = 17.8/5.7 Hz, 1H); 2.49 (dd, J = 18.3/9.6 Hz, 1H)	10	37.4	3.04 (dd, J = 17.6/5.8 Hz, 1H); 2.74 (dd, J = 18.0/9.2 Hz, 1H)
11	169.8 (171.2)	58.9 (58.1)		11	163.9	
12	110.9 (112.1)	58.8 (58.7)		12	117.0	
13	178.9 (179.9)	67.3 (67.4)		13	170.0	
14	106.2 (107.4)	67.5 (66.6)		14	114.0	
15	160.4 (161.5)	71.3 (71.2)		15	158.4	
16	102.1 (103.2)	71.3 (71.9)	6.31 (s, 1H)	16	100.2	6.78 (s, 1H)
17	163.5 (164.8)	66.9 (62.1)	10.70 (s, 10H)	17	161.4	10.86 (s, 10H)
18	113.7 (114.6)	62.1 (62.4)	6.44 (s, 1H)	18	119.5	6.78 (s, 1H)
19	143.0 (144.2)	41.7 (42.3)		19	142.0	
20	22.2 (22.6)	42.1 (42.5)	2.64 (s, 3H)	20	22.6	2.77 (s, 3H)

[a] ^1H and ^{13}C NMR spectra were recorded in DMSO-d_6 (400 MHz for ^1H and 100 MHz for ^{13}C). [b] Carbons are labeled according to their number in the polyketide backbone (Figure 2). [c] Data in parentheses were recorded in DMF-d_7 to identify the C-10 peak covered by DMSO-d_6 peaks.

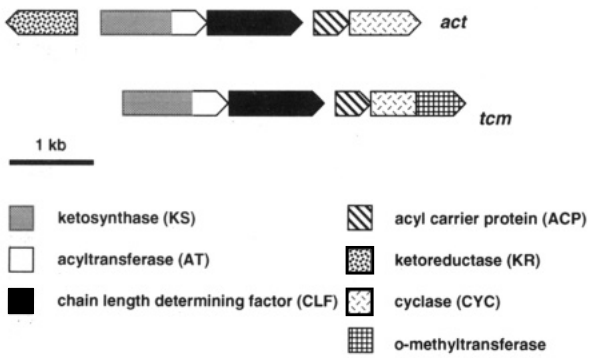

FIGURE 1: *act* and *tcm* PKS gene clusters. Each "minimal" PKS includes a ketosynthase/putative acyl transferase (KS/AT), a chain length determining factor (CLF), and an acyl carrier protein (ACP); the *act* cluster also contains a ketoreductase (KR). The AT has been postulated to transfer the starter unit from coenzyme A to the KS, which catalyzes the Claisen condensation between the starter (or growing polyketide) acyl thioester and the extender (malonyl) thioester on the ACP; this rests on the finding of a putative acyl transferase active site in the deduced sequence of the gene product. The KR reduces a specific carbonyl (C-9) of the actinorhodin polyketide backbone. The gene clusters also encode a cyclase (CYC), involved in cyclization of the nascent polyketide backbone; however, the *tcm* cyclase (TcmN) is unusual, since it is similar to the *act* (and other) cyclases only in the N-terminal half of the polypeptide, while its C-terminal half resembles *o*-methyltransferases (Summers et al., 1992). The C-terminal half of the *act* and other related cyclases (but not TcmN) have been postulated to possess a dehydratase function (Sherman et al, 1991), but an amino acid sequence similarity between the N- and C-terminal halves has already been described (Bibb et al., 1994).

act KR; Figure 1) reduced polyketide chains of different lengths, probably after the complete polyketide chain had been synthesized (Bartel et al., 1990); (v) regardless of chain length, this ketoreductase reduced the C-9 carbonyl, counting from the carboxyl end (Bartel et al., 1990); (vi) the regiospecificity of the first cyclization was controlled by the KS/AT and/or the CLF; and (vii) a specific cyclase (the *act* CYC; Figure 1), responsible for catalyzing the second cyclization reaction, could evidently discriminate between intermediates of different chain lengths and degrees of reduction, based upon its inability to act on certain unnatural substrates.

We describe here the structures of two novel diastereomeric polyketides produced by a recombinant strain expressing the "minimal" *tcm* PKS (i.e., KS/AT + CLF + ACP), the *act* KR, and the *act* CYC (Figure 1). This strain (CH999/pRM37) had already been shown to produce a novel polyketide, RM20 (**3**) (McDaniel et al., 1993a), whereas a related strain (CH999/pSEK15), lacking the *act* KR gene, produced another novel polyketide, SEK15 (**4**) (Fu et al., 1994). As expected, RM20 and SEK15 were derived from singly reduced and completely unreduced decaketide backbones, respectively. Furthermore, both backbones underwent the first cyclization (intramolecular aldol condensation) with the same regiospecificity. However, the two molecules exhibited very different patterns of subsequent cyclizations. Whereas the singly cyclized RM20 precursor was converted into a fused ring structure via one aldol condensation and two hemiacetal formation reactions, the singly cyclized SEK15 precursor underwent an aldol condensation and a lactonization, giving rise to a molecule with three unfused rings. Since neither of these cyclization patterns resembled those observed in the natural products of the *tcm* and *act* PKSs [tetracenomycin C (**2**) and actinorhodin (**1**), respectively], the *act* cyclase was assumed to lack catalytic activity on a longer polyketide chain. In order to identify the degrees of freedom available *in vivo* to a nascent polyketide chain for cyclizing in the absence of an active cyclase, the culture media of these two recombinant strains were examined for other relatively abundant polyketides. The molecules reported here possess unique features, which provide new insights into the mechanisms of catalysis by multifunctional PKSs.

MATERIALS AND METHODS

Bacterial Strains and Plasmids. Polyketides produced by recombinant *Streptomyces coelicolor* CH999/pRM37 (McDaniel et al., 1993a) were structurally analyzed in this study. The relevant biosynthetic enzymes encoded by pRM37 are the *tcm* ketosynthase/putative acyl transferase (KS/AT),

the *tcm* chain length determining factor (CLF), the *tcm* acyl carrier protein (ACP), and the *act* ketoreductase (KR); genes for the *act* cyclase (CYC) and a putative dehydratase from the *act* cluster (*act*IV) are also present on pRM37 but have been shown not to influence production of the molecules reported here (McDaniel et al., 1994).

Production and Purification of RM20b (5) and RM20c (6). Except for the production of [$^{13}C_2$]acetate-enriched polyketides, CH999/pRM37 was grown on R2YE agar plates (Hopwood et al., 1985) rather than in liquid medium because of the more abundant production of metabolites on agar media. The strain was grown on 30 agar plates (~34 mL/plate) at 30 °C for 7 days. The agar was chopped and extracted with ethyl acetate/methanol (4:1) in the presence of 1% acetic acid (3 × 800 mL). The solvent was removed under vacuum. The residue was applied to a Florisil column (Fisher Scientific) and eluted with ethyl acetate/ethanol/acetic acid (17:2:1). The products were futher purified on a Beckman HPLC using a preparative C-18 reverse-phase column (mobile phase, acetonitrile/water = 1:9 to 3:2 over a period of 53 min). The amounts of RM20b and RM20c recovered were 70 and 10 mg, respectively.

[1,2-$^{13}C_2$]Acetate Feeding Experiments. Two 2-L flasks, each containing 400 mL of modified NMP medium (Strauch et al., 1991), were inoculated with spores of *S. coelicolor* CH999/pRM37. At 72 and 96 h postinoculation, 50 mg of sodium [1,2-$^{13}C_2$]acetate (Aldrich) was added to each flask. After 120 h, the cultures were extracted with two 500-mL volumes of ethyl acetate/1% acetic acid. The organic phase was kept, and the products were purified as described above. Approximately 3 mg of RM20b was obtained. ^{13}C NMR data (62 016 scans in DMSO-d_6 and 60 608 scans in DMF-d_7) indicated approximately 1–2% enrichment (estimated by comparing peak areas to the natural abundance ^{13}C peak area). The amount of labeled RM20c obtained from this experiment was insufficient for ^{13}C NMR analysis.

Mass and NMR Spectroscopy and Optical Rotation Diffractometry. High-resolution mass spectra (HRMS) were recorded on a VG ZAB-ZSE mass spectrometer under fast atom bombardment (FAB) conditions. NMR spectra were recorded on a Varian XL-400. ^{13}C spectra were acquired with continuous broad-band proton decoupling. All compounds were dissolved in DMSO-d_6 or DMF-d_7 (Sigma, 99+ atom % D), and spectra were referenced internally to the solvent. Hydroxyl resonances were identified by adding D_2O (Aldrich, 99 atom % D) and checking for disappearance of signal. Optical rotatory dispersion (ORD) studies were performed on a Jasco DIP-360 digital polarimeter.

RESULTS

Structures of RM20b (5) and RM20c (6). The two novel compounds, RM20b and RM20c, were discovered in the culture medium of CH999/pRM37, which had previously yielded RM20 (3). The relative quantities of the three compounds recovered were 3:7:1 (RM20/RM20b/RM20c). ^1H and ^{13}C NMR spectra suggested that RM20b and RM20c were diastereomers, each containing a pyrone moiety similar to that present in mutactin (Zhang et al., 1990) and SEK4 (Fu et al., 1994). Optical rotations ($[\alpha]_D^{20}$) were found to be +210.8° for RM20b (EtOH, 0.55%) and +78.0° for RM20c (EtOH, 0.33%). Sodium [1,2-$^{13}C_2$]acetate feeding experiments confirmed that the carbon chain of RM20b (and by inference RM20c) was derived from 10 acetate units. Deuterium exchange studies were carried out in order to identify ^1H NMR peaks corresponding to potential hydroxyl groups on both RM20b and RM20c. Proton coupling constants were calculated from the results of ^1H NMR and one-dimensional decoupling experiments. In particular, the

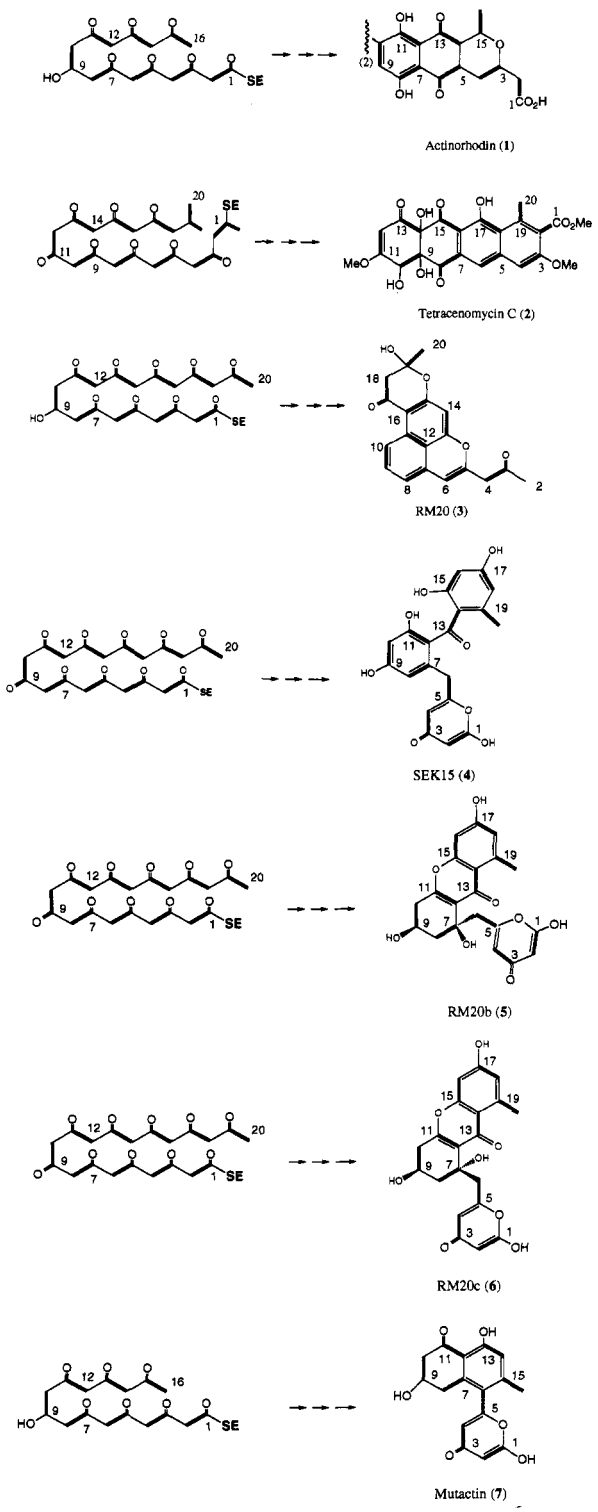

FIGURE 2: Polyketides (right) and deduced backbones (left) synthesized by PKSs. Actinorhodin and tetracenomycin C are the natural products of *S. coelicolor* and *Streptomyces glaucescens* containing the entire *act* and *tcm* gene clusters, respectively. RM20, RM20b, and RM20c are congeners from the culture medium of *S. coelicolor* CH999 (which lacks the *act* cluster) carrying pRM37 (McDaniel et al., 1993a; this work); this plasmid contains genes for the minimal *tcm* PKS (KS/AT, CLF, and ACP) together with the *act* KR and the *act* CYC (Figure 1). The producer of SEK15 is identical to CH999/pRM37 but lacks the *act* KR (Fu et al., 1994). Mutactin is a shunt product produced by a mutant of *S. coelicolor* lacking *act* CYC activity (Zhang et al., 1990).

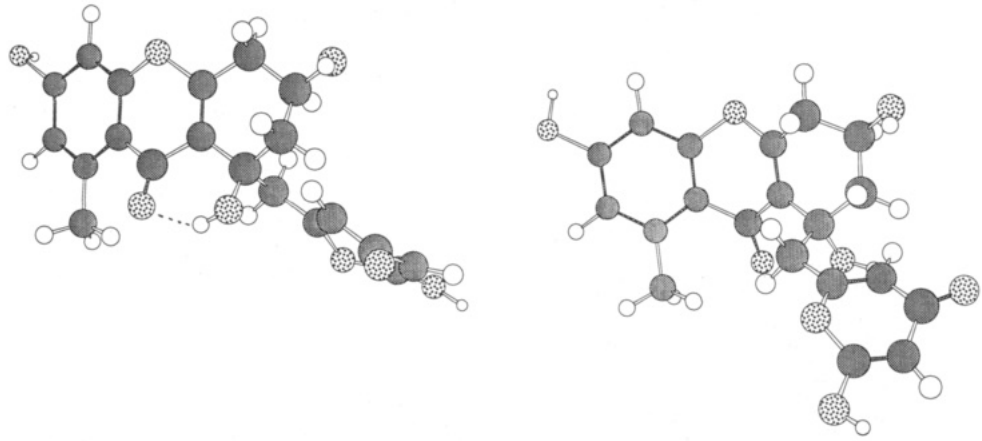

FIGURE 3: Three-dimensional structures of RM20b (left) and RM20c (right). The hydrogen bond in RM20b between the C-13 carbonyl and the C-7 hydroxyl is shown by the dashed line.

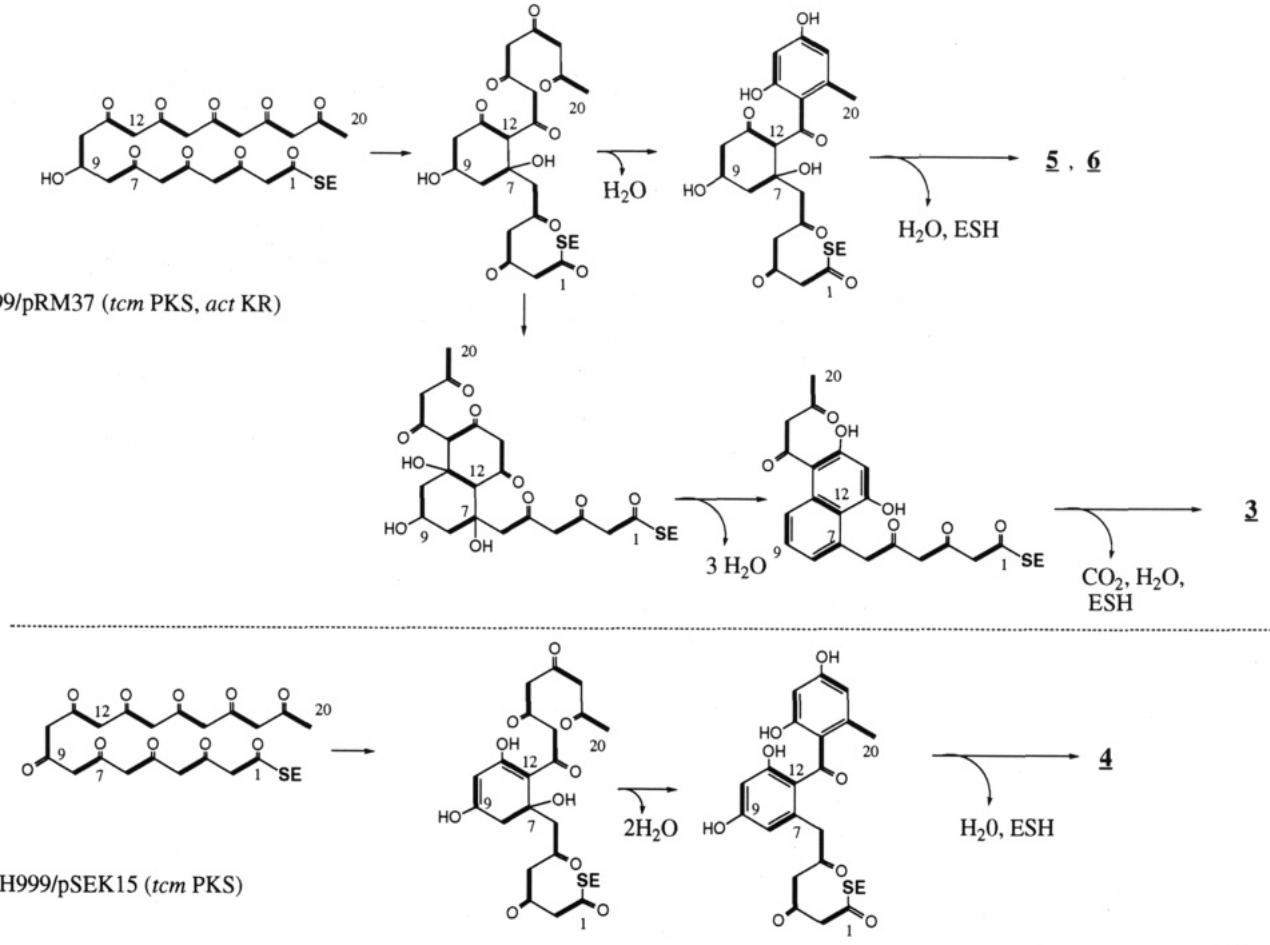

FIGURE 4: Comparison of the biosynthetic pathways of RM20, RM20b, RM20c, and SEK15. RM20, RM20b, and RM20c are metabolites produced by CH999/pRM37, which expresses the *tcm* PKS along with the *act* KR. SEK15 is produced by CH999/pSEK15, which is identical to CH999/pRM37, except for the absence of *act* KR activity.

coupling pattern in the upfield region of the spectrum indicated a five-proton spin system of two methylene groups surrounding a central carbinol methine proton, similar to that observed in mutactin (Zhang et al., 1990). High-resolution fast atom bombardment (FAB) mass spectroscopy gave molecular weights of 519.0056 ($M + Cs^+$) for RM20b and 387.1070 ($M + H^+$) for RM20c, consistent with $C_{20}H_{18}O_8$ ($M + Cs^+$ 519.0056 and $M + H^+$ 387.1080). On the basis of the above data, the structures **5** and **6** were assigned to RM20b and RM20c, respectively. (The stereochemistry was deduced as described below.) Final ^{13}C peak assignments for RM20b were made using data from sodium [1,2-$^{13}C_2$]acetate feeding experiments, whereas assignments for RM20c were made in comparison with those of RM20b.

Determination of Stereoconfiguration of RM20b and RM20c. As summarized in Table 1, the coupling constants between H-9 and the geminal protons on C-8 were 12.1 and 2.5 Hz for RM20b (12.2 and 2.2 Hz for RM20c). Likewise, the coupling constants between H-9 and the geminal protons on C-10 were 9.6 and 5.7 Hz for RM20b (9.2 and 5.8 Hz for RM20c). These values are typical of a $J_{a,a}$ ($J_{9a,8a}$ or $J_{9a,10a}$) and $J_{a,e}$ ($J_{9a,8e}$ or $J_{9a,10e}$) coupling pattern and argue in favor of an axial position for H-9 in both RM20b and RM20c. This would also be consistent with the axial assignment of the

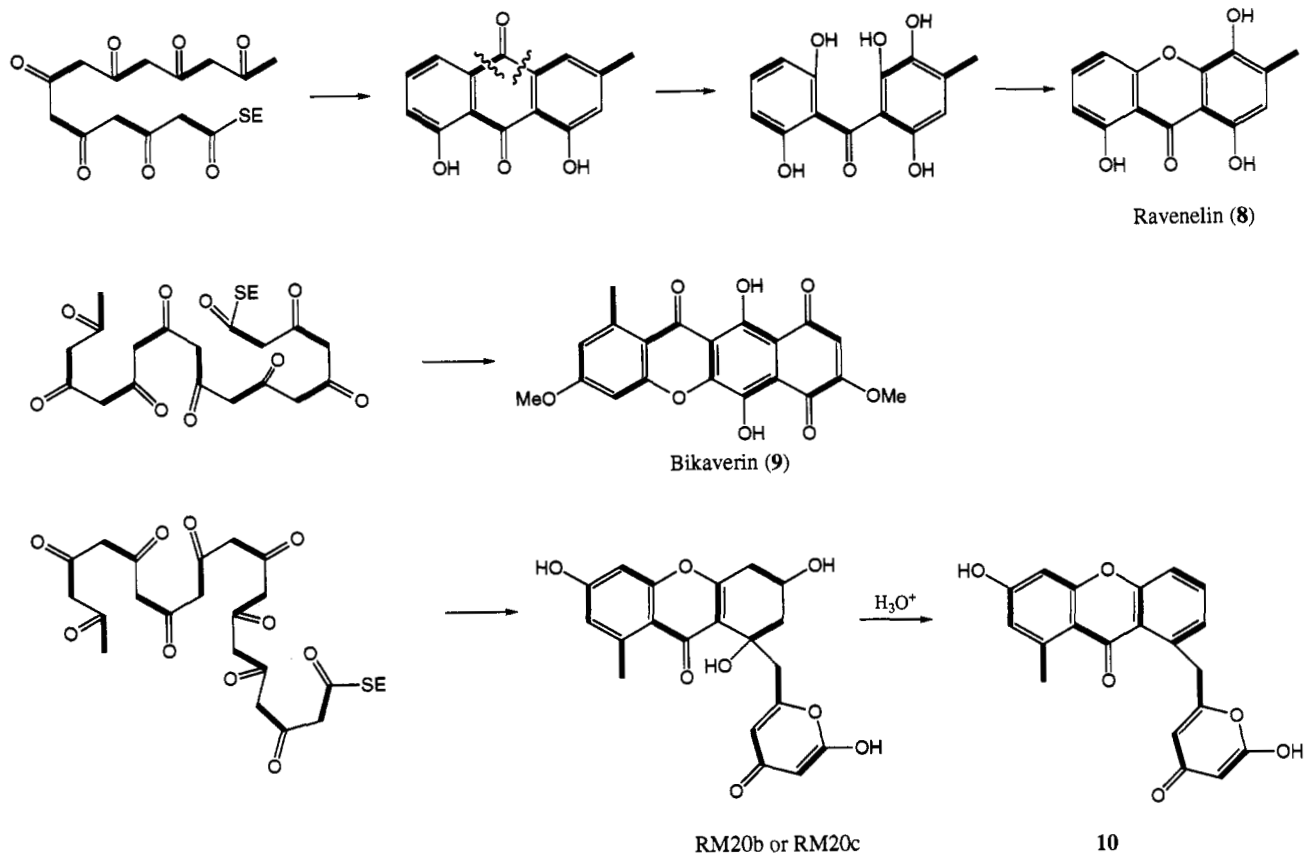

FIGURE 5: Comparison of the biosynthesis of xanthones (ravenelin and bikaverin) with that of RM20b and RM20c [in part after O'Hagan (1991)].

corresponding proton in mutactin (**7**) (Zhang et al., 1990). In contrast, the chemical shifts of the C-7 hydroxyls on the two molecules were drastically different (16.18 ppm in RM20b and 6.14 ppm in RM20c). These values suggest the existence of a hydrogen bond between the C-7 hydroxyl and a suitably positioned acceptor atom in RM20b, but not in RM20c. The most likely candidate acceptor atoms for such hydrogen bonding are the C-13 carbonyl oxygen in the conjugated pyrone ring system or the bridge oxygen in the isolated pyrone ring. The latter possibility is unlikely, since it would be unable to discriminate between the two diastereomers. Furthermore, comparison of ^{13}C NMR spectra of RM20b and RM20c revealed that the greatest differences between the two molecules were in the chemical shifts of the carbons that make up the conjugated pyrone ring (+5.9, −6.1, +8.9, −7.8, and +2.0 ppm for C-11, C-12, C-13, C-14, and C-15, respectively). Such a pattern of alternating upfield and downfield shifts can be explained by the fact that the C-7 hydroxyl is hydrogen bonded to the C-13 carbonyl, since hydrogen bonding would be expected to reduce the electron density around C-11, C-13, and C-15 but increase the electron density around C-12 and C-14. To confirm the C-7/C-13 hydrogen bond assignment, the exchangable protons in RM20b and RM20c were replaced with deuterium (by incubating in the presence of D_2O), and the samples were analyzed by ^{13}C NMR. The C-13 peak in RM20b, but not in RM20c, underwent an upfield shift (1.7 ppm), which can be explained by a weaker C-7/C-13 noncovalent bond in RM20b when hydrogen is replaced with deuterium. In order to form a hydrogen bond with the C-13 carbonyl, the C-7 hydroxyl of RM20b must occupy the equatorial position. Thus, it can be inferred that the C-7 and C-9 hydroxyls are on the same face (*syn*) of the conjugated ring system in the major isomer (RM20b), whereas they are on opposite sides (*anti*) in the minor isomer (RM20c). These two relative configurations are shown in Figure 3. (The absolute stereochemistry was not determined.) Both RM20b and RM20c were converted into the corresponding xanthone (**10**) by treatment with acid.

DISCUSSION

The structures of RM20b and RM20c reveal an additional degree of freedom that can be exploited for the rational generation of novel polyketides through the manipulation of gene structure and organization. In particular, from a comparison of RM20 (**3**) with RM20b (**5**) and RM20c (**6**), it can be seen that, in the absence of an active cyclase, the same polyketide precursor can undergo cyclization *in vivo* in more than one way. As shown in Figure 4, a C-11/C-16 aldol condensation gives rise to RM20 (**3**), whereas an alternative C-14/C-19 aldol condensation results in RM20b (**5**) and RM20c (**6**) formation. Biosynthesis of each of these three products requires the C-11 carbonyl to be predominantly in the keto form. Presumably this is facilitated by the C-9 ketoreduction catalyzed by the *act* KR. In contrast, CH999/pSEK15, which expresses the *tcm* PKS but lacks the *act* KR, produces SEK15 (**4**) (Fu et al., 1994). The inability of this molecule to form a xanthone suggests that the C-11 carbonyl undergoes facile enolization in the absence of a C-9 ketoreduction (Figure 4).

The conjugated ring system of RM20b and RM20c is interesting, since it can be easily dehydrated under acidic conditions to yield a xanthone moiety, which is found in several bacterial and eucaryotic aromatic polyketides (O'Hagan, 1991; Carter et al., 1989). Xanthones are generally formed by the oxidative rearrangement of an anthraquinone skeleton, as in ravenelin (**8**) (Figure 5; Birch et al., 1976) and simaomicin (Carter et al., 1989). However, in rare cases they can be

produced directly from a folded polyketide chain, as in bikaverin (**9**) (Figure 5; McInnes et al., 1975). The polyketide backbones of RM20b and RM20c are folded in a manner that is more similar to the case of bikaverin than that of ravenelin or simaomicin. To the best of our knowledge, the dehydrated form of RM20b and RM20c (**10**; generated under acidic conditions) represents the first example of a bacterial xanthone produced by the direct folding of polyketide chains. Thus, our results demonstrate that genetic engineering of bacterial PKSs can provide access to biosynthetic pathways which are not commonly observed in naturally occurring bacteria.

ACKNOWLEDGMENT

We are grateful to Koji Ichinose and Peter Revill for helpful comments on the manuscript.

REFERENCES

Bartel, P. L., Zhu, C. B., Lampel, J. S., Dosch, D. C., Connors, N. C., Strohl, W. R., Beale, J. M., & Floss, H. G. (1990) *J. Bacteriol. 172*, 4816–4826.

Bibb, M. J., Sherman, D. H., & Hopwood, D. A. (1994) *Gene 142*, 31–39.

Birch, A. J., Baldas, J., Hlubucek, J. R., Simpson, T. J., & Westerman, P. W. (1976) *J. Chem. Soc., Perkin Trans. I*, 898–904.

Carter, G. T., Goodman, J. J., Torrey, M. J., Borders, D. B., & Gould, S. J. (1989) *J. Org. Chem. 54*, 4321–4323.

Fu, H., Ebert-Khosla, S., Hopwood, D. A., & Khosla, C. (1994) *J. Am. Chem. Soc. 116*, 4166–4170.

Hopwood, D. A., Bibb, M. J., Chater, K. F., Kieser, T., Bruton, C. J., Kieser, H. M.,

Lydiate, D. J., Smith, C. P., Ward, J. M., & Schrempf, H. (1985) *Genetic Manipulation of Streptomyces. A Laboratory Manual*, The John Innes Foundation, Norwich, U.K.

Katz, L., & Donadio, S. (1993) *Annu. Rev. Microbiol.* 47, 875–912.

McDaniel, R., Ebert-Khosla, S., Hopwood, D. A., & Khosla, C. (1993a) *Science 262*, 1546–1550.

McDaniel, R., Ebert-Khosla, S., Hopwood, D. A., & Khosla, C. (1993b) *J. Am. Chem. Soc. 115*, 11671–11675.

McDaniel, R., Ebert-Khosla, S., Fu, H., Hopwood, D. A., & Khosla, C. (1994) *Proc. Natl. Acad. Sci. U.S.A.* (in press).

McInnes, A. G., Smith, D. G., Walter, J. A., Vining, L. C., & Wright, J. L. C. (1975) *J. Chem. Soc. Chem. Commun.*, 66–68.

O'Hagan, D. (1991) *The Polyketide Metabolites*, Ellis Horwood, Chichester, U.K.

Sherman, D. H., Bibb, M. J., Simpson, T. J., Johnson, D., Malpartida, F., Fernandez-Moreno, M., Martinez, E., Hutchinson, C. R., & Hopwood, D. A. (1991) *Tetrahedron 47*, 6029–6043.

Summers, R. G., Wendt-Pienkowski, E., Motamedi, H., & Hutchinson, C. R. (1992) *J. Bacteriol. 174*, 1810–1820.

Zhang, H. L., He, X. G., Adefarati, A., Gallucci, J., Cole, S. P., Beale, J. M., Keller,

P. J., Chang, C. J., & Floss, H. G. (1990) *J. Org. Chem. 55*, 1682–1684.